

Linear Voltage Controlled Oscillator Implementation in Electronically Variable Immittances

Koushick MATHUR^{1,*}, Palaniandavar VENKATESWARAN², and
Rabindranath NANDI²

¹UIT-Burdwan University, Department of Electronics & Communication Engineering

²Jadavpur University, Department of Electronics & Telecommunication Engineering

E-mails: kousik.mathur@gmail.com*, pvwn@ieee.org,

robsilverju@yahoo.com

* Corresponding author

Abstract. New realization schemes of electronically tunable inductor (L) and Frequency-Dependent Negative Resistance (D) type immittances using a *Current Feedback Amplifier* (CFA) and *Multiplication Mode Current Conveyor* (MMCC) composite *active building block* (ABB) are proposed. Applications of the immittances to the design of selective filters and LC-type *linear voltage controlled quadrature oscillator* (LVCQO) are presented. Experimental results based on PSPICE simulation and hardware design for a linear range of oscillation frequency ($f_o \sim 13.6\text{MHz}$) with satisfactory phase-noise figure on the oscillator wave response had been verified. Effects of the *Active Building Block* (ABB)–nodal imperfections are analyzed to be insignificant. The new ideas in this article are two types of immittance functions realizable in the same topology; appropriate frequency-domain selective responses are also presented with experimentation results.

Key-words: *Current Feedback Amplifier* (CFA); linear voltage control oscillator; quadrature; selective filter; synthetic inductor/FDNR.

1. Introduction

Design implementation of the inductor (L) and *Frequency Dependent Negative Resistance* (FDNR) (D) [1, 2] type active immittance functions has been receiving considerable research interest presently. Albeit quite a number of passive tuned L and D immittance synthesis schemes have been proposed in the recent past [3–6], their electronically variable versions are quite few,

Table 1. Summary of recent immittance functions

Ref.	ABB Used	Immittance type	Tunability by	Select frequency (MHz)
[7]	DO-CCCII	L	I_b	0.1
[8]	CCTA	D	I_b	0.14
[9]	DVCCTA	L and D	g_m	2.5
[10]	VDVTA	L and D	g_m	1.2
[11]	OTA	L	g_m	0.2
[12]	VDTRA	D	$\sqrt{I_b}$	0.1
[13]	CFA-4 and OTA-2	L	$\sqrt{I_b}$	4.0
[14]	ETDVCCTA	L and D	V	5.0
[15]	CFOA OTA	C-Multiplier	I_b	7.0
[16]	Ex-CCCII (using 5-CFAs)	L and D	$\sqrt{I_b}$	0.01 (filter response)
[17]	CFA-Multiplier	L and D	V	6.3
[18]	Multiplier-loop	-	V	13.2
Proposed	MMCC-CFA	D and L	V	5.1

2. Immittance Functions

The proposed immittance function realization schemes are shown in Fig. 1; the device node equations are $I_z = \alpha_{1,2} I_x$, $V_w = \delta_{1,2} V_z$ and $V_x = \beta_2 V_y$, $V_x = \beta_1 k V V_y$; $k \approx 1/\text{volt.d.c.}$ [19] where k is the multiplication constant; the subscripts 1 & 2 are for the MMCC and CFA respectively while $C_{z1,2}$ and $C_{y1,2}$ are the device parasitic capacitances ($3.3 < C_{y,z}$ (pF) < 5.7) [22]. The port coefficients, assuming device roll-off poles, may be expressed as $\alpha_{1,2} \approx (1 - \varepsilon_{i,1,2})/(s\tau_{i,1,2} + 1)$, $\beta_2 \approx (1 - \varepsilon_{v,2})/(s\tau_{i,1,2} + 1)$, $\delta_1 \approx (1 - \varepsilon_{o1})/(s\tau_{i,o1} + 1)$. The dc-gain errors are quite low ($\varepsilon \ll 1$).

The proposed realization circuit is shown in Fig. 1; derivation of the input impedances (Z_i) is evaluated as shown in Table-2. These are derived as $Z_i = Z_1 Z_3 / (k V Z_2)$ assuming ideal ABB elements ($\varepsilon \ll 1$; $\alpha \approx \beta \approx \delta = 1$). With appropriate choice of the port RC-components, the proposed immittances are derived as illustrated in Table 2.

The modified input impedance in Fig. 1 is

$$\hat{Z}_i = Z_i / \alpha_2 \beta_2 \alpha_1 \delta_1 \quad (1)$$

where: $\alpha_{1,2} \approx (1 - \varepsilon_{i,1,2})/(s\tau_{i,1,2} + 1)$, $\beta_2 \approx (1 - \varepsilon_{v2})/(s\tau_{v2} + 1)$, and $\delta_1 \approx (1 - \varepsilon_{o1})/(s\tau_{o1} + 1)$; since the rolloff poles appear closely at relatively high-frequency-range, we may assume $\tau_{i,v,z} \approx \tau \equiv 1/\omega_p$ that yields

$$\alpha_2 \beta_2 \alpha_1 \delta_1 \approx 1 / \{ (s\tau)^4 + (4s\tau)^3 + (6s\tau)^2 + 4s\tau + 1 \} \quad (2)$$

Neglecting higher order-terms and writing $s\tau = j\omega\tau \equiv j\omega/\omega_p \approx ju$ for the frequency-domain, the modified L-value is obtained, assuming $u \ll 1$, as

$$\hat{L}/L = \delta L = 1 / \sqrt{\{16u^2 + 1\}} @ \angle \arctan(4u) \quad (3)$$

Table 2. Realization of L and D elements in Fig. 1

Type	Component selection	Immittance
a.	$Z_{1,3} = R_{1,3}$ $Z_2 = 1/sC$	$Z_i = sL$ and $L = R_1 R_3 C / kV \approx CR^2 / kV$
b.	$Z_{1,3} = 1/sC_{1,3}$ $Z_2 = R$	$Z_i = 1/s^2 D$ $D = C_1 C_3 R (kV) \approx RC^2 (kV)$

Hence effects of the device rolloff poles are quite negligible. Similar derivations for the D-element may also be derived, given by

$$\tilde{D}/D = \delta D = \sqrt{\{16u^2 + 1\}} @ \perp - \arctan(4u) \quad (4)$$

Hence effects of the device rolloff poles are quite negligible. Similar derivations for the D-element may also be derived, given by

3. Effects of Parasitic Capacitances

The effects of device parasitic capacitances are analyzed as

$$\tilde{Y}_{iL} = \{sC_p + (1/s)\tilde{L}\} \quad (5)$$

where $C_p \approx C_{z1} + C_{y2}$. Therefore

$$\tilde{L} = L(1 + \mu) \approx L; \mu \approx C_{z2}/C \ll 1 \quad (6)$$

and

$$\tilde{Y}_{iD} = \{sC_p + s^2\tilde{D}\} \quad (7)$$

where $\tilde{D} = D/(1 + jp)$; $p = \omega/\omega_{z2}$; $\omega_{z2} = 1/RC_{z2}$.

$$i.e. \tilde{D}(\omega) = D/(p^2 + 1) \approx D; p \ll 1 \quad (8)$$

The measurement indicates $C_{y1}, C_{z1}, 2 \sim 3.7pF$, *i.e.* with usual R-values in $k\Omega$ range, one gets $f_{z2} \sim 57MHz$; hence 3-dB rolloff for constant nominal value of D in Eq. (7) appears at quite a higher corner frequency. The useful frequency-range ($p \ll 1$) of the FDNR applications has therefore been assumed constant for the proposed design applications here.

4. Filter Design Applications

The proposed L and D immittances are next utilized for the design of new LC-type bandpass (BP) and rD-type band-reject (BR) filters as shown in Fig. 2 (a) and (b), respectively. The design equations are summarized in Table 3. Effects of parasitic capacitors ($C_{z,p}$) on stability factor S_F have been investigated as shown in Table 4.

Effects of the port errors ($\varepsilon_{i,v,z} \ll 1$) on filter circuit parameters *i.e.*, quality factor (Q) and pole frequency (ω_o) are quite negligible, given by

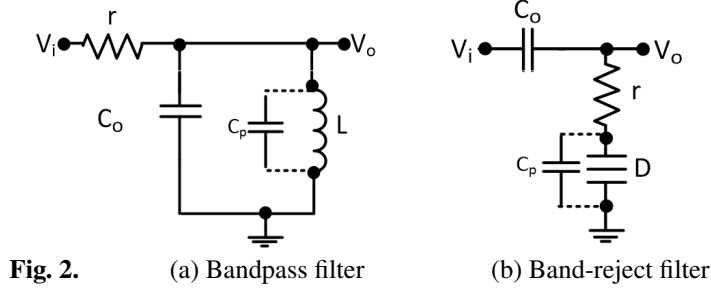


Fig. 2. (a) Bandpass filter (b) Band-reject filter

$$Q'_{bp} \approx Q\sqrt{1-\varepsilon_T} \quad \text{and} \quad Q'_{br} \approx \frac{Q}{\sqrt{1-\varepsilon_T}} \quad (9)$$

$$\omega'_{bp} \approx \omega_o\sqrt{1-\varepsilon_T} \quad \text{and} \quad \omega'_{br} \approx \frac{\omega_o}{\sqrt{1-\varepsilon_T}} \quad (10)$$

where $\varepsilon_T = \varepsilon_{i1} + \varepsilon_{i2} + \varepsilon_{v1} + \varepsilon_{o2}$.

Table 3. BP and BR filter design schemes

Fig. 2	Filter Transfer Function (F)	Filter parameters	Measured Values
	LC-type BPF :		
(a)	$F_{bp} = \frac{s \frac{L}{r}}{s^2 LC(1+\sigma) + s(\frac{L}{r}) + 1}$ where $\sigma = \frac{C_p}{C} \ll 1$; $C_p = C_{y1} + C_{z2}$	$\omega_o = \frac{1}{C} \sqrt{\frac{kV}{rR}}$ and $Q \approx \frac{r}{\omega_o L}$	$f_o \approx 5MHz$ $Q \approx 4.6$
	rD-type BRF:		
(b)	$F_{br} = \frac{s^2 + s \frac{C_p}{D} + \frac{1}{rD}}{s^2 + s \left\{ \frac{C_p}{D} + \frac{1}{rC_o} \right\} + \frac{1}{rD} \left[1 + \frac{C_p}{C_o} \right]}$ $\approx \frac{s^2 + \frac{1}{rD}}{s^2 + s \frac{1}{rC_o} + \frac{1}{rD}}$ where $C_p/D \approx \frac{C_p}{C^2} / RV^2 \ll 1$; as $C_p \ll C$	$\omega_o = \frac{1}{C_o \sqrt{kVRr}}$ and $Q \approx \frac{C_o}{C} \sqrt{\frac{r}{kVR}}$	$f_o \approx 4.5MHz$ $Q \approx 10$
Capacitors : $C_{y,z(1,2)} \sim 3.6 \text{ pF}$			

Table 4. Measured Value of Parasitic Capacitors : $C_{y,z(1,2)} \sim \text{pF}$

Filter Type	Parasitic components	$S_F u = \omega/\omega \approx 1$
LC-type BPF	Capacitors ($C_{z,p}$) $\sigma = C_p/C_o \ll 1$ $\mu = C_{z1}/C \ll 1$	$S_F = 2 \frac{r}{R} \sqrt{\frac{kVC_o(1+\sigma)}{C(1+\mu)}}$ $\approx 2 \frac{r}{R} \sqrt{\frac{kVC_o}{C}} \gg 1$ $as \frac{r}{R} \gg 1, C \geq C_o$
rD-type BRF	Capacitors (Cp) $\sigma = C_p/C_o \ll 1$ $\varphi = C_p/C \ll 1$	$S_F = \frac{2\sqrt{\frac{1+\sigma}{rD}}}{\left[\frac{C_p}{D} + \frac{1}{rC_o}\right]} \approx \frac{2}{\varphi} \sqrt{\frac{kVR}{r}} \gg 1$ $as \frac{C_o}{C} \gg 1, R \geq r$

Effects of relative change in ω_o may be expressed [38] as $(\Delta\omega_o/\omega_o) \approx -\{(\partial R/R) + (\partial C/C)\}$ for

the change of temperature of 0°C to 100°C, which shows variation of component as $\partial C/C = (-)1.9\%$ and $\partial R/R \leq (+)2.1\%$ (max)[39–40]; hence $\Delta\omega_o/\omega_o \sim 0$.

5. Voltage Control Oscillator (VCO) Design

The analysis of the state-of-the-art indicates quite a number of electronically tunable *Quadrature Oscillators* (QO) were proposed recently in [27–38], where only a few exhibits a linear f_o -tuning law as listed in Table 5. Some of these are tuned by the device bias current (I_b) or transconductance (g_m). Next, VTI circuit in Fig. 1 has been modified as shown in Fig. 3, to implement the VCOs by putting input node- V_i at ground. Here the input impedance (Z_i) at node V_o , derived as $Z_i = Z_1 Z_3 / [Z_2 (kV)^2]$.

The characteristic equation (CE) of these proposed oscillators in Fig. 3 can be obtained as [37] following the continuous-time model, in terms of

$$Z_L + Z_i = 0 \quad (11)$$

In (11), choosing $Z_X = 1/sC_o$ and r , in combination with $Z_i = s\tilde{L}$ and $1/s^2\tilde{D}$ respectively, the CE of LC and rD type Voltage Control Oscillators yields

$$\frac{1}{sC_o} + s\tilde{L} = 0 \quad \text{and} \quad r + \frac{1}{s^2\tilde{D}} = 0 \quad (12)$$

Table 5. Summary of electronically tunable QOs

Ref.	ABB	f_o (MHz)	Tuning by	Linear Tuning Law	THD%
[27]	CDTA	1.73	$\sqrt{I_b}$	No	3
[28]	VDIBA	8.5	$\sqrt{I_b}$	No	2.2
[29]	DVCCTA	3.18	$\sqrt{I_b}$	No	–
[30]	DVCCTA	1.6	$\sqrt{I_b}$	No	2
[31]	CCTA	1.7	$\sqrt{I_b}$	No	0.3
[32]	CCCTA	3.1	Ib	No	4.28
[33]	ETDVCCTA	9	V	Yes	3.3
[34]	CFTA	5.1	$\sqrt{g_m}$	No	2~4.5
[35]	VTCCTA	9.9	V	Yes	1.5
[36]	CDBA-2	0.13	MOS switch	No	3.4
[37]	CFA-1 & Multiplier	12	V	Yes	–
[38]	DX-MOCCII*	5.62	MOS bias voltage	No	3.1
Proposed	MMCC-CFA	~ 13.6	V	Yes	3.6

Hence these frequency of oscillation (FO), ω_{oL} and ω_{oD} for LC-type and rD-type oscillator respectively may be derived using the performance specifications of the oscillation frequencies written as

$$\omega_{oL} = \frac{1}{\sqrt{\tilde{L}C_o}} \approx \frac{kV}{\sqrt{C_o CR_1 R_3}} \quad (13)$$

as $\tilde{L} = L(1(\mu)) \approx L = \frac{CR_1R_3}{(kV)^2}$ as $Z_{1,3} = R_{1,3}, Z_2 = 1/sC, \mu \ll 1$.

Similarly, selecting $Z_{1,3} = 1/sC_{1,3}$ and $Z_2 = R_1$,

$$\omega_{oD} = \frac{1}{\sqrt{r\tilde{D}}} \approx \frac{1}{kV\sqrt{C_1C_3R_1r}} \quad (14)$$

as $\tilde{D} = D(1(p)) \approx D = R_1C_1C_3(kV)^2$ and $p \ll 1$

The desired computation of the oscillator-parameters is derived in terms of (13) and (14) as per requirement of the oscillation-frequency range. This computation is exemplified in Section 6.

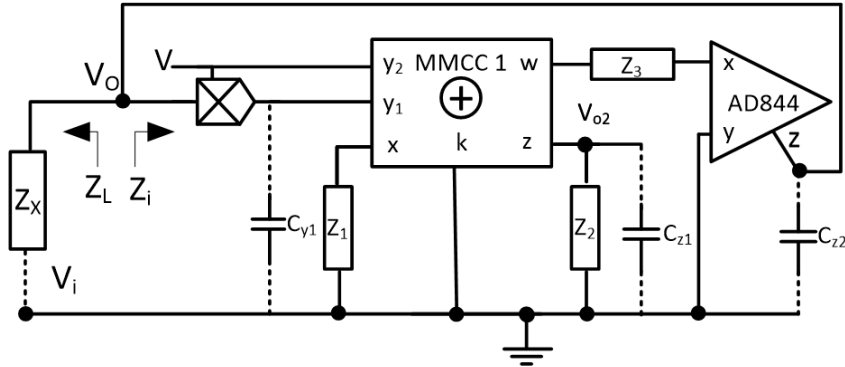


Fig. 3. Modified immittance function based Voltage Controlled Oscillator.

Hence the objectives of the control are clearly outlined by Equations (13) and (14) that exhibit the oscillation frequency (f_o) is tunable by the multiplier control voltage (V), where the LC-type oscillator yields a linear voltage control law with quadrature property. Several linear and nonlinear controllers with successful applications in various fields and those applications are closely related to the process treated here [44–46].

6. Experimental Results

The BP, BR filter and VCO responses are measured from the hardware design with d.c. supply voltage ± 5 volt and $k=1/V$ of the MMCC, using thin film technology based passive SMD components to alleviate the temperature sensitivity issue; these are shown in Fig. 4. The bandpass (BP) filter shows its high selectivity response at center frequency ~ 5 MHz in Fig. 4 (a) with the design value as $r = 2.7K\Omega, R=820\Omega, C = C_o = 56pF$ at $V=2.1$ volt d.c. Similarly, the bandreject (BR) filter response has been obtained with the center frequency 4.4 MHz with $r = R = 820\Omega, C = 47pF, C_o = 470pF$ at $V = 0.91$ volt d.c. The THD variation at this pole frequency for a wide range of applied input sinusoidal peak-peak amplitude has been verified for both filters in Fig. 4 (b).

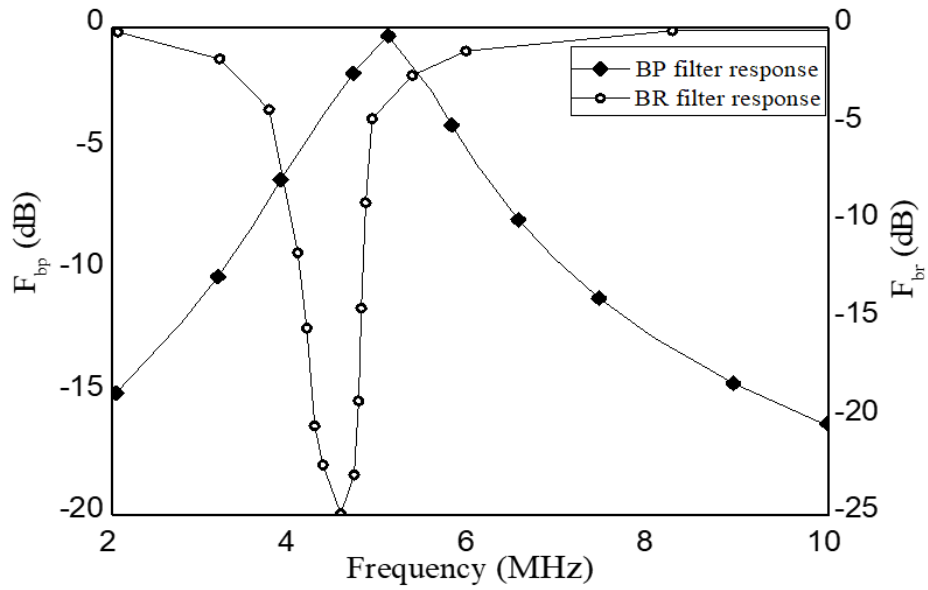


Fig. 4a. Filter response of the filter circuit in Fig. 2.

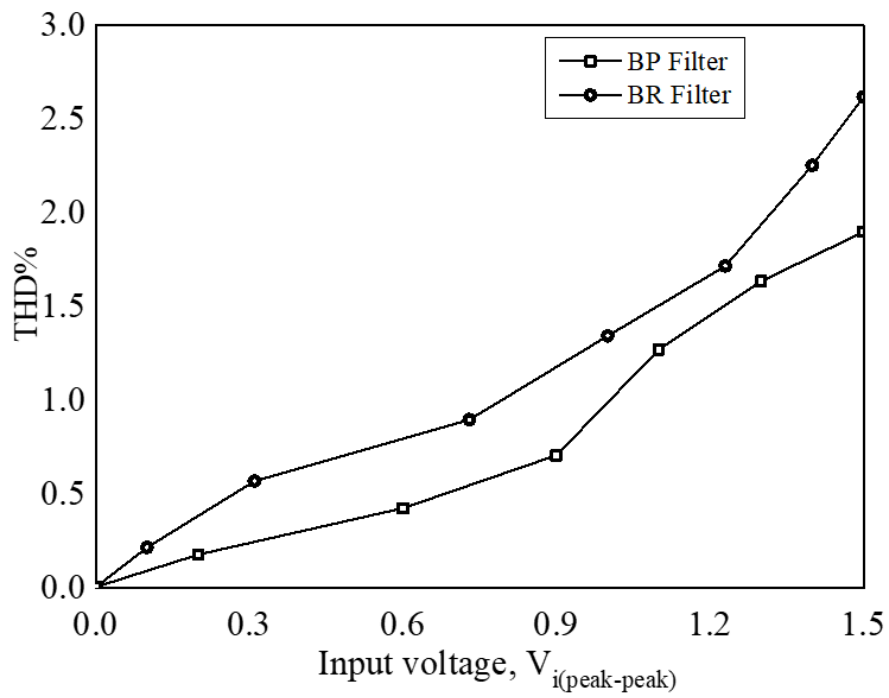


Fig. 4b. THD response of the filter circuit in Fig. 2.

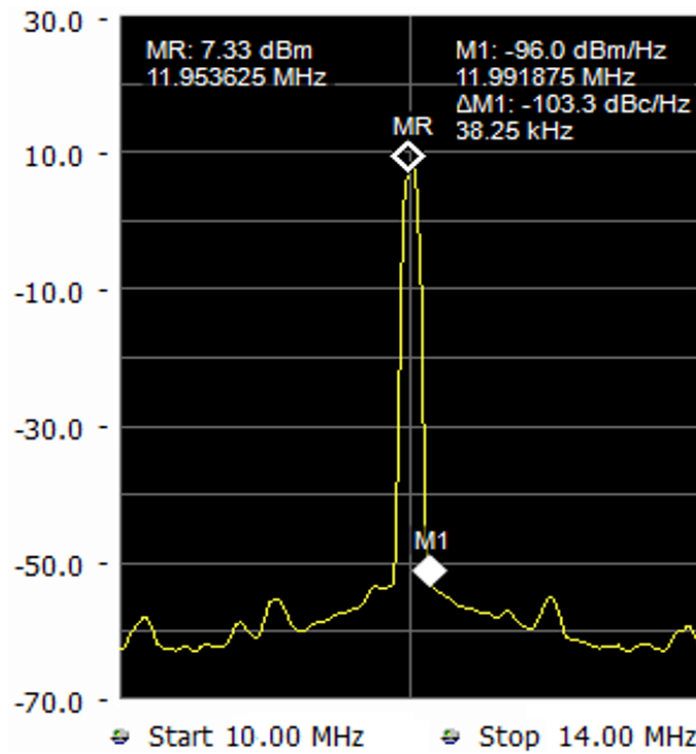


Fig. 4c. Spectral response and phase-noise of LC-type linear voltage control quadrature-oscillator.

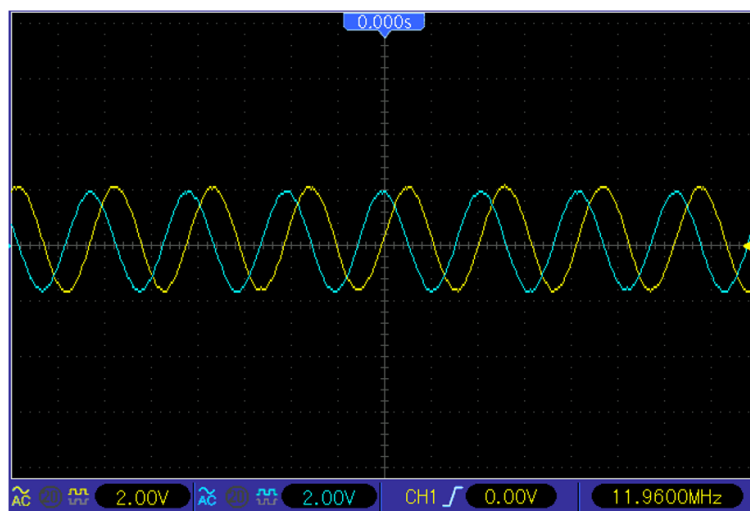


Fig. 4d. QO waveform of LVCQO (V_{o-} - yellow trace and V_{o1-} - blue trace) in Fig. 3 .

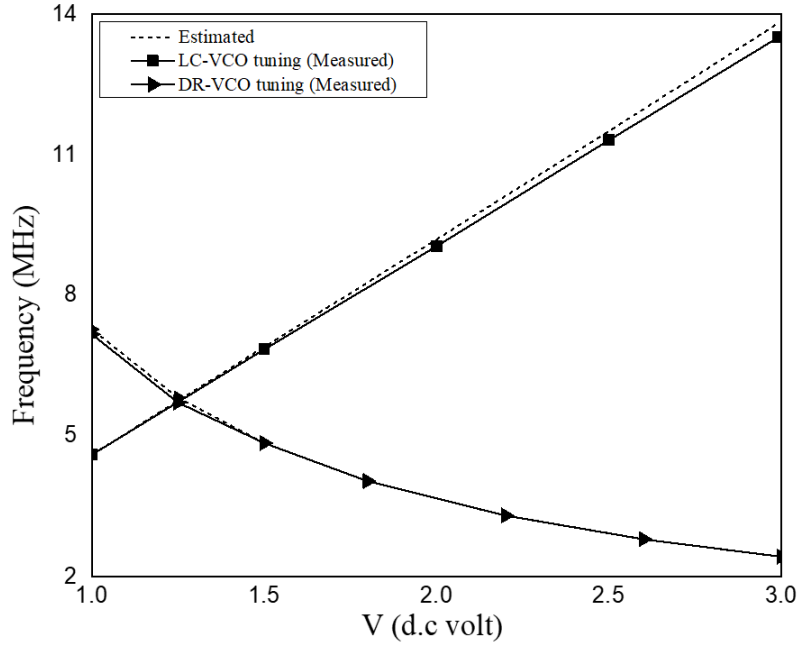


Fig. 4e. Tuning law of LC and DR type VCO .

The LC-type VCO response at $V=2.6$ volt d.c the spectrum at $f_o \sim 12\text{MHz}$ and its phase noise of (-103) dBc/Hz at 38 KHz offset at node- V_o has been shown in Fig. 4 (c). Hence an enhanced frequency with improved spectrum quality has been observed in comparison to the [27]. Thereafter its quadrature waveform in between node- V_o and V_{oq} in Fig. 3 at $f_o \sim 12\text{MHz}$ with 1.5% and 1.7% THD, have been obtained as shown in Fig. 4 (d). The tuning law of the proposed LC and rD-type VCO circuit has been experimentally verified with suitably chosen the values of $R1=R3=470\Omega$, $C=C_o=74\text{pF}$ and $R1=r=470\Omega$, $C1=C3=47\text{pF}$ respectively as depicted in Fig. 4 (e). The linearity error (Δ) in oscillator response had been evaluated following the definition [41]. In Fig. 4 (e), the measured slope of the LC oscillator for the range 4.6MHz \sim 13.6MHz is $(13.56-4.61)\text{MHz}/(3-1)\text{V.d.c.} = 4.48\text{MHz/V} \equiv \epsilon_2$. Calculated slope $\epsilon_1 = 4.6\text{MHz/V.d.c.}$ Hence $\Delta = (\epsilon_1 - \epsilon_2)/\epsilon_1 \equiv 2.6\%$.

7. Conclusions

A new electronically variable immittance function circuit implementation scheme was presented for the design of electronically tunable L and D type immittances; subsequently measured responses of the frequency selective BP, BR filters along with LC and rD type VCQs are examined. Experimental results on linear QO- response with satisfactory frequency-stability factor and phase-noise figure have been included. Wave harmonic distortion of the quadrature sinusoid signal and the linearity error is quite low for the designed QO. Along with this, a highly selective voltage tunable BP and BR filter with low THD has been obtained. Effects of CFA-device parasitic components are negligible on the frequency-stability (S_F) figure.

In the context of the proposed work, of some recent and classical papers [44–46] on several linear and nonlinear controllers with successful applications in various fields, these useful applications are closely related to the process treated in this work. The response of the proposed circuit-designs has been compared with recent research literature that exhibits a minimum component based compact design with better results on the proposed implementation.

Acknowledgement. Authors would like to thank the editor and unknown reviewers for their helpful comments and suggestions.

References

- [1] L. T. BRUTON, *Network transfer function using the concept of frequency-dependent negative resistance*, IEEE Transactions on Circuit Theory **16**(3), pp. 406–408, 1969.
- [2] U. KUMAR, *Current conveyors: A review of the state of the art*, IEEE Circuits & Systems Magazine **3**(1), pp. 10–14, 1981.
- [3] R. NANDI, *Active inductances using current conveyors & their applications in a simple bandpass filter realization*, Electronics Letters **14**(12), pp. 373–375, 1978.
- [4] R. NANDI, S. L. SANYAL and T. K. BANDYOPADHYA, *Low-sensitivity multifunction active circuits using CFA-based supercapacitor*, International Journal of Electronics **93**(10), pp. 689–698, 2006.
- [5] M. T. ABUELMATTI, *New grounded immittance functions using single current feedback operational amplifier*, Analog Integrated Circuits and Signal Processing **71**(1), pp. 95–100, 2012.
- [6] M. DOGAN and E. YUCE, *CFOA-based new grounded inductor simulator and its applications*, Microelectronics Journal **90**, pp. 297–305, 2019.
- [7] M. SAGBAS, U. E. AYTEN, H. SEDEF and M. KOKSAL, *Electronically tunable floating inductance simulator*, International Journal of Electronics and Communications (AEU) **63**(5), pp. 423–427, 2009.
- [8] A. JANTAKUN, *A simple grounded FDNR and capacitance simulator based on CCTA*, International Journal of Electronics and Communications (AEU) **69**(6), pp. 950–957, 2015.
- [9] H. ALPASLAN, *A modified VDVT and its applications to floating simulators and a quadrature oscillator*, Microelectronics Journal **51**, pp. 1–14, 2016.
- [10] R. NANDI, S. DAS and P. VENKATESWARAN, *Floating lossless immittance functions using DVCCTA*, International Journal of Electronics Letters **4**(1), pp. 117–126, 2016.
- [11] S. SIRIPONGDEE and W. JAIKLA, *Electronically controlled grounded inductance simulators using single commercially available IC:LT1228*, International Journal of Electronics and Communications (AEU) **76**, pp. 1–10, 2017.
- [12] M. C. DIKBAS and U. E. AYTEN, *Voltage differencing transresistance amplifier & its application: floating FDNR simulator circuit*, International Journal of Electronics **105**(10), pp. 1716–1720, 2018.
- [13] N. KUMAR, J. VISTA and A. RANJAN, *A tuneable active inductor employing DXCCTA: Grounded and floating operation*, Microelectronics Journal **90**(1), pp. 901–911, 2019.
- [14] R. NANDI, K. MATHUR and P. VENKATESWARAN, *Quadrature voltage control oscillator with a linear tuning law*, IET Circuits, Devices & Systems **12**(2), pp. 157–163, 2018.
- [15] M. A. AL-ABSI and M. T. ABUELMATTI, *A novel tunable grounded positive & negative impedance multiplier*, IEEE Transactions on Circuit And Systems-II **66**(6), pp. 924–927, 2019.
- [16] D. AGARWAL and S. MAHESWARI, *Electronically tunable grounded immittance simulators using an EX-CCII*, International Journal of Electronics **107**(10), pp. 1625–1648, 2020.

- [17] K. MATHUR and R. NANDI, *Voltage tunable immittance functions: Linear voltage-controlled quadrature oscillator implementation*, International Journal of Electronics Letters DOI: 10.1080/21681724.2021.2025441, 2022.
- [18] K. MATHUR, P. VENKETESEWARAN and R. NANDI, *A linear VCO using single-CFA and analog multipliers*, Journal of Circuits Systems & Computers **31**(6), paper 2250111, 2022.
- [19] Y. S. HWANG, W. H. LIU, S. TU and J. J. CHEN, *New building block: multiplication mode current conveyor*, IET Circuits, Devices & Systems **3**(1), pp. 41–48, 2009.
- [20] Analog Devices Datasheet: AD-835: 250MHz, 4 quadrant voltage multiplier; file#D00883-0-12/14(E), 2017.
- [21] Intersil-Datasheet: file2477.5; Sept.1998 & file 2863, 1999.
- [22] Analog Devices: Linear Product Databook Products Databook, MA, USA, 1990.
- [23] Macromodel of ADD844AN in PSPICE Library (Microsym) Corporation, MA, USA, 1990.
- [24] R. NANDI, T. K. BANDYOPADHY and S. K. SANYAL, *Selective filter and sinusoid oscillators using CFA transimpedance pole*, Circuits, Systems & Signal Processing **28**, pp. 349–359, 2009.
- [25] A. A. TAMMAM, K. HAYATLEH, M. BEN-ESMAEL, N. TETZOPOULOS and C. SEBU, *Critical review of the circuit architecture of CFOA*, International Journal of Electronics **101**(4), pp. 441–451, 2014.
- [26] S. J. G. GIFT and B. MAUNDY, *Improving the bandwidth gain-independence and accuracy of the current feedback amplifier*, IEEE Transactions on Circuits And Systems **52**(3), pp. 136–139, 2005.
- [27] J. JIN and C. WANG, *Single CDTA-based current mode quadrature oscillator*, International Journal of Electronics and Communications (AEU) **66**(11), pp. 933–936, 2012.
- [28] N. HERNCSAR, S. MINAEI, J. KOTON E. YUCE and K. VRBA, *New resistorless and electronically tunable realization of dual-output VM allpass filter using VDIBA*, Analog Integrated Circuits and Signal Processing **74**, pp. 141–154, 2013.
- [29] H. P. CHEN, S. F. WANG and M. Y. HSIEH, *Tunable current mode and voltage mode quadrature oscillator using DVCCTA*, IEICE Electronics Express **11**(13), pp. 1–6, 2014.
- [30] N. PANDEY and R. PANDEY, *Approach for third-order quadrature oscillator realization*, IET Circuits, Devices & Systems **9**(3), pp. 161–171, 2015.
- [31] A. JANTAKUN, *A simple grounded-FDNR and capacitance simulator based on CCTA*, International Journal of Electronics and Communications (AEU) **69**(6), pp. 950–957, 2012.
- [32] W. TANGSRIRAT, O. CHANNUMSIN and T. PUKKALANUN, *Single current controlled sinusoidal oscillator with current and voltage output using single current controlled transconductance amplifier and grounded passive elements*, Revue Roumaine des Sciences Techniques, Srie lectrotechnique et nerg-tique **60**(2), pp. 175–184, 2015.
- [33] R. NANDI, K. MATHUR and P. VENKATESWARAN, *Quadrature voltage control oscillator with a linear tuning law*, IET Circuits, Devices & Systems **12**(2), pp. 157–163, 2017.
- [34] N. KUMNGERN and F. KHATIB, *Current mode universal filter and quadrature oscillator using current controlled current follower transconductance amplifiers*, Analog Integrated Circuits and Signal Processing **100**(2), pp. 235–248, 2019.
- [35] R. NANDI, K. MATHUR and P. VENKATESWARAN, *Electronically tunable immittances with applications to LP, BP, HP filter and VCO implementation*, International Journal of Electronics Letters **9**(1), pp. 65–75, 2019.
- [36] S. S. BORAH, A. SINGH, M. GHOSH and A. RANJAN, *Electronically tunable higher-order quadrature oscillator employing CDBA*, Microelectronics Journal **108**, pp. 1–8, 2021.

- [37] K. MATHUR, P. VENKATESWARAN and R. NANDI, *A linear electronically tunable sinusoid oscillator*, IEICE Electronics Express **17**(22), pp. 1–3, 2020.
- [38] A. KUMAR, A. K. KHUSWAHA and S. K. PAUL, *Electronically tunable mixed-mode quadrature oscillator using DX-MOCCII*, Journal of Circuits Systems and Computers **30**(1), 2150006, 2021.
- [39] K. KUROKAWA, *Some basic characteristics of broadband negative resistance oscillator circuits*, The Bell System Technology Journal **48**(6), pp. 1937–1955, 1969.
- [40] M. HRIBSECK and R. W. NEWCOMB, *VCO controlled by one variable resistor*, IEEE Transactions on Circuits and Systems **23**(3), pp.166–169, 1976.
- [41] <http://www.vishay.com/docs/26033/gentechinfofilm.pdf>. Accessed: 2017.
- [42] <http://www.vishay.com/docs/20043/crcwhpe3.pdf>. Accessed: 2016.
- [43] A. BARBAIE–FISHARI and P. ROMBOUTS, *Highly linear VCO for use in VCO–ADCs*, Electronics Letters **52**(4), pp. 268–269, 2016.
- [44] R.–E. PRECUP and S. PREITL, *PI-fuzzy controllers for integral plants to ensure robust stability*, Information Sciences **177**(2007), pp. 4410–4429, 2007.
- [45] C. A. IORDACHE and M. BODEA, *Analysis and design of a high-efficiency current-mode buck converter with I2C controlled output voltage*, Romanian Journal of Information Science & Technology **23**(2), pp.188–203, 2020.
- [46] R.–C. ROMAN, R.–E. PRECUP, E.–L. HEDREA, S. PREITL, I. A. ZAMFIRACHE, C.–A. BOJAN-DRAGOS and E. M. PETRIU, *Iterative feedback tuning algorithm for tower crane systems*, Procedia Computer Science **199**, pp. 157–165, 2022.